

Syntheses and Characterization of Organo-Group 14 Cobaloxime Compounds

Alan M. Stolzenberg,* Sarah R. Workman, Jessica E. Gutshall, Jeffrey L. Petersen, and Novruz Akhmedov

Department of Chemistry, West Virginia University, P.O. Box 6045, Morgantown, West Virginia 26506

Received February 8, 2007

Reactions of cobaloxime $\text{Na}[(t\text{-BuPy})\text{Co}(\text{DH})_2]$ with Ph_3ECl ($\text{E} = \text{Si}, \text{Ge}, \text{Sn}, \text{and Pb}$) were investigated. Metal–metal bonded complexes $(t\text{-BuPy})\text{Co}(\text{DH})_2\text{EPh}_3$ were isolated for $\text{E} = \text{Sn}$ and Pb . $(t\text{-BuPy})\text{Co}(\text{DH})_2\text{SnPh}_3 \cdot (\text{C}_2\text{H}_5)_2\text{O}$, $\text{C}_{39}\text{H}_{52}\text{CoN}_5\text{O}_5\text{Sn}$, crystallized in the monoclinic space group $P2_1/c$ ($Z = 4$) with unit cell dimensions $a = 11.6443(6)$ Å, $b = 15.6085(8)$ Å, $c = 22.6354(12)$ Å, $\beta = 96.634(1)^\circ$, and $V = 4086.4(4)$ Å³ at 295(2) K. The structure resembled those of six-coordinate alkyl cobaloxime complexes and had Co–N_{py} and Co–Sn distances of 2.056(2) and 2.5568(3) Å, respectively. $(t\text{-BuPy})\text{Co}(\text{DH})_2\text{PbPh}_3$, $\text{C}_{35}\text{H}_{42}\text{CoN}_5\text{O}_4\text{Pb}$, crystallized in the monoclinic space group $P2_1/n$ ($Z = 4$) with unit cell dimensions $a = 15.0104(7)$ Å, $b = 15.7693(8)$ Å, $c = 16.6230(8)$ Å, $\beta = 114.348(1)^\circ$, and $V = 3584.8(3)$ Å³ at 295(2) K. The complex was nearly isostructural with the Sn analogue and had Co–N_{py} and Co–Pb distances of 2.049(2) and 2.6191(4) Å, respectively. Coupling of the ortho phenyl protons to the spin 1/2 isotopes of Sn and of Pb was a characteristic feature of the ¹H NMR spectrum. Additional, longer range couplings were observed for the Pb complex and for both complexes in the ¹³C NMR. Metal–metal bonded complexes were not obtained for $\text{E} = \text{Si}$ or Ge . The products isolated in the latter case were the hydride Ph_3GeH and the cobalt(II) complex $(t\text{-BuPy})\text{Co}(\text{DH})_2 \cdot \text{C}_{17}\text{H}_{27}\text{CoN}_5\text{O}_4$, which crystallized in the orthorhombic space group $Pbcn$ ($Z = 8$). Unit cell dimensions were $a = 17.9821(11)$ Å, $b = 9.7449(6)$ Å, $c = 22.7374(15)$ Å, and $V = 3984.4(4)$ Å³ at 295(2) K. The five-coordinate complex had $\text{Co–N}_{\text{py}} = 2.096(2)$ Å and was dimeric in the lattice.

Introduction

The existence of the metal–metal-bonded, cobalt octaethylporphyrin complex $\text{Co}^{\text{III}}(\text{OEP})\text{SnPh}_3$ was unexpected.¹ However, the exceptional inertness of this Co–Sn -bonded complex compared to that of related Co–C -bonded alkyl cobalt(III) porphyrin complexes was a more significant surprise. $\text{Co}^{\text{III}}(\text{OEP})\text{SnPh}_3$ survives anaerobic chromatography on alumina and silica supports. It is air stable in solution at room temperature for extended times in most solvents and decomposes by homolysis very slowly at 120 °C in toluene. Anaerobic heating in this solvent causes only a few percent decomposition to $\text{Co}^{\text{II}}(\text{OEP})$ after 12 h. Similarly, photolysis of the complex for extended times affords only partial conversion to products resulting from Co–Sn bond cleavage. The Co–Sn bond cleaves rapidly and completely, though, when oxidized by I_2 or by electrochemical means.

It is unclear whether the unexpected inertness of $\text{Co}^{\text{III}}(\text{OEP})\text{SnPh}_3$ to thermal and photochemical decomposition results from thermodynamic or kinetic factors. Scheme 1 shows a homolytic mechanism for decomposition that involves a solvent-caged radical pair. The starting complex could be thermodynamically stable if the Co–Sn bond dissociation energy was large relative to the Sn–X bond(s) and possibly Co–X bond(s) in the thermolysis product(s). In the context of Scheme 1, a large Co–Sn bond dissociation energy would result in a small rate of homolysis (i.e., small k_h). A second possibility is that a high cage efficiency leads to a very low probability of escape of the $\text{Ph}_3\text{Sn}^\bullet$ radical from the solvent cage ($k_c \gg k_d$).^{2,3} Last, the inertness could result from the persistent radical effect,^{4–6} which occurs when

* To whom correspondence should be addressed. E-mail: astolzen@wvu.edu.

(1) Cao, Y.; Petersen, J. L.; Stolzenberg, A. M. *Inorg. Chem.* **1998**, *37*, 5173–5179.

(2) Garr, C. D.; Finke, R. G. *J. Am. Chem. Soc.* **1992**, *114*, 10440–10445.

(3) Koenig, T. W.; Hay, B. P.; Finke, R. G. *Polyhedron* **1988**, *7*, 1499–1516.

(4) Fischer, H. *J. Am. Chem. Soc.* **1986**, *108*, 3925–3927.

(5) Fischer, H. *Chem. Rev.* **2001**, *101*, 3581–3610.

(6) Daikh, B. E.; Finke, R. G. *J. Am. Chem. Soc.* **1992**, *114*, 2938–2943.

Scheme 1



one of the radical species formed by bond homolysis does not self-terminate or react with radical traps. In the current case, irreversible loss of some $\text{Ph}_3\text{Sn}^\bullet$ radical through dimerization or reaction with a trap like a halogenated solvent or O_2 would lead to a persistent concentration of the stable porphyrin metalloradical $\text{Co}^{\text{II}}(\text{OEP})$. This will suppress the concentration of the $\text{Ph}_3\text{Sn}^\bullet$ free radical and make the trapping of subsequently formed $\text{Ph}_3\text{Sn}^\bullet$ free radical to afford the caged pair and ultimately $\text{Co}^{\text{III}}(\text{OEP})\text{SnPh}_3$ faster than either self-termination of the $\text{Ph}_3\text{Sn}^\bullet$ free radical or irreversible radical trapping reactions ($k_{-1(\text{soln})}[\text{Co}(\text{P})][\text{SnPh}_3] \gg 2k_{\text{self}}[\text{SnPh}_3]^2$ or $k_T[\text{SnPh}_3][\text{T}]$). The effectiveness of low concentrations of cobalt(II) porphyrin and macrocycle compounds in modifying the chemistry of free radicals was amply demonstrated in studies of catalytic chain transfer during free-radical polymerizations.^{7,8}

The unavailability of Co–E bond dissociation energy data for Group 14 elements with E heavier than carbon leaves unresolved the extent to which a strong Co–Sn bond is responsible for the inertness of $\text{Co}^{\text{III}}(\text{OEP})\text{SnPh}_3$. The Co–C bond in alkyl cobalt porphyrin,⁹ cobaloxime,^{10,11} and cobalamin^{12–15} complexes has a BDE that ranges from 18 to 37 kcal/mol. The BDE depends on alkyl group and axial base and is typically >30 kcal/mol for methyl or primary alkyls. It is not apparent what factors could cause a Co–Sn bond to be substantially stronger than a Co–C bond. Moreover, the partial conversion of $\text{Co}^{\text{III}}(\text{OEP})\text{Sn}(\text{C}_4\text{H}_9)_3$ to $\text{Co}^{\text{III}}(\text{OEP})\text{C}_4\text{H}_9$ during chromatography or on standing in solution suggests that some Co–Sn cleavage occurs under these conditions.¹ The Co–Sn bond strength in $\text{Co}^{\text{III}}(\text{OEP})\text{-Sn}(\text{C}_4\text{H}_9)_3$ should be roughly comparable to that in $\text{Co}^{\text{III}}(\text{OEP})\text{SnPh}_3$. In fact, substitution of alkyl for aryl groups would be expected to lead to minor strengthening of the Sn–Co bond, if it follows the trends for Sn–H and Sn–X bond strengths.¹⁶

The lack of Co–E bond dissociation energy data for E other than carbon reflects, in large part, the few complexes known that contain Co–E bonds to the heavier Group 14 elements. The number is particularly small for complexes that contain cobalt coordinated by four nitrogen donors. Aside from the $\text{Co}^{\text{III}}(\text{OEP})\text{SnR}_3$ complexes discussed above, the sole examples that we have found in the literature are a

homologous series of cobaloxime complexes $(\text{Py})\text{Co}(\text{DH})_2\text{ER}_3$ (where DH = monoanion of dimethylglyoxime and E = Si, Ge, Sn, and Pb) that were synthesized by Schrauzer.^{17,18} The complexes were reported to have good thermal and moderate air stability (for E = Sn and Pb), but neither the properties nor reactivity of these complexes was thoroughly investigated. Later work by other investigators demonstrated that the 4-*t*-butylpyridine analogue of the triphenylstannylcobaloxime complex could be used as a radical initiator.^{19,20}

The $(\text{Py})\text{Co}(\text{DH})_2\text{ER}_3$ compounds present an opportunity both to investigate Co–E bond dissociation energies as functions of the identities of the Group 14 element E and the R group and to investigate whether the inertness of $\text{Co}(\text{OEP})\text{SnPh}_3$ is a property unique to that complex or a more general phenomenon. Such investigations would require that the compounds both be accessible and have reactivity suitable for measurement of bond dissociation energies either by thermochemical or kinetic methods. In this paper, we report a reinvestigation of the syntheses of organo-Group 14 cobaloxime compounds and the characterization of those that are accessible in our hands. The reactivity of these complexes will be examined in a subsequent paper.

Experimental Section

Materials and Methods. All reactions, recrystallizations, and sample manipulations were carried out under subdued lights and a nitrogen atmosphere using Schlenk techniques or in a Vacuum Atmospheres Co. Drybox unless noted otherwise. $\text{Co}(\text{DH})(\text{DH}_2)\text{-Cl}_2$,²¹ (4-*t*-BuPy)Co(DH)₂Cl,²¹ and (4-*t*-BuPy)Co(DH)₂(*n*-C₄H₉)²² were prepared by literature methods. All compounds and solvents used were reagent grade or the best grade available. Chlorotriphenyllead (90%) was obtained from Aldrich. Chlorotriphenyltin (95%) was purchased from Acros and from Aldrich. Triphenylchlorogermane (95%) and triphenylchlorosilane (95%) were obtained from Gelest, Inc. Diethylether and tetrahydrofuran (THF) were deoxygenated and dried by passage through a column of activated alumina. CDCl_3 and C_6D_6 were passed through a small bed of neutral grade I alumina and deoxygenated immediately prior to use. ¹H NMR spectra were recorded on a JEOL Eclipse (270.17 MHz) or a Varian Inova 600 (599.667 MHz) spectrometer. Unambiguous structural assignments were achieved using one- and two-dimensional NMR techniques including APT, DEPT, HETCOR, TOCSY1D, gHMQC, and gHMBC. EPR spectra were recorded on a Bruker EMX spectrometer equipped with an ER 4131VT variable-temperature accessory. Magnetic susceptibility

- (7) Gridnev, A. A.; Ittel, S. D.; Fryd, M.; Wayland, B. B. *Organometallics* **1996**, *15*, 222–235.
 (8) Gridnev, A. A.; Ittel, S. D. *Chem. Rev.* **2001**, *101*, 3611–3659.
 (9) Geno, M. K.; Halpern, J. *J. Am. Chem. Soc.* **1987**, *109*, 1238–1240.
 (10) Halpern, J. *Polyhedron* **1988**, *7*, 1483–1490.
 (11) Toscano, P. J.; Seligson, A. L.; Curran, M. T.; Skrobitt, A. T.; Sonnenberger, D. C. *Inorg. Chem.* **1989**, *28*, 166–168.
 (12) Halpern, J.; Kim, S.-H.; Leung, T. W. *J. Am. Chem. Soc.* **1984**, *106*, 8317–8319.
 (13) Kim, S.-H.; Chen, H. L.; Feilchenfeld, N.; Halpern, J. *J. Am. Chem. Soc.* **1988**, *110*, 3120–3126.
 (14) Hay, B. P.; Finke, R. G. *J. Am. Chem. Soc.* **1986**, *108*, 4820–4829.
 (15) Martin, B. D.; Finke, R. G. *J. Am. Chem. Soc.* **1992**, *114*, 585–592.
 (16) Nolan, S. P.; Porchia, M.; Marks, T. J. *Organometallics* **1991**, *10*, 1450–1457.

- (17) Schrauzer, G. N.; Kratel, G. *Angew. Chem., Int. Ed. Engl.* **1965**, *4*, 146–147.
 (18) Schrauzer, G. N.; Kratel, G. *Chem. Ber.* **1969**, *102*, 2392–2407.
 (19) Tada, M.; Kaneko, K. *J. Org. Chem.* **1995**, *60*, 6635–6636.
 (20) Tada, M.; Hanaoka, Y. *J. Organomet. Chem.* **2000**, *616*, 89–95.
 (21) Trogler, W. C.; Stewart, R. C.; Epps, L. A.; Marzilli, L. G. *Inorg. Chem.* **1974**, *13*, 1564–1570.
 (22) Jameson, D. L.; Grzybowski, J. J.; Hammels, D. E.; Castellano, R. K.; Hoke, M. E.; Freed, K.; Basquill, S.; Mendel, A.; Shoemaker, W. *J. J. Chem. Ed.* **1998**, *75*, 447–450.

measurements were performed on a Johnson–Matthey susceptometer. Magnetic moments were calculated using diamagnetic corrections.

(4-*t*-Butylpyridine)triphenyltincoloxime, (4-*t*-BuPy)Co(DH)₂SnPh₃·Et₂O.¹⁹ (4-*t*-BuPy)Co(DH)₂Cl (0.95 g, 2.1 mmol) was suspended in 20 mL of methanol in a 50 mL Schlenk flask. The flask was deaerated, back-filled with nitrogen gas, and placed in an ice bath. Addition of 0.50 mL of a 4.4 M aqueous NaOH (2.2 mmol contained NaOH) to the stirred suspension resulted in dissolution of the solid to afford a golden-yellow solution. The solution turned the deep blue-black color characteristic of cob(I)-aloximes upon addition of NaBH₄ (80 mg, 2.1 mmol). After stirring for 15 min, 0.76 g of solid chlorotriphenyltin (1.9 mmol based on 95% purity) was added under nitrogen flush and the flask was covered with aluminum foil to exclude light. The ice bath was removed after 15 min of reaction, and the flask was permitted to warm to room temperature and stir overnight. During this time, the solution slowly turned a orange-red color and a fine, yellow-brown precipitate formed. The contents of the flask were transferred (aerobically) to a separatory funnel that contained 25 mL of distilled water and 16 mL of CH₂Cl₂. An additional 8 mL of CH₂Cl₂ was used to dissolve any remaining solid in the reaction flask, and the resulting solution was added to the separatory funnel. The CH₂Cl₂ layer was separated from the aqueous layer, dried with NaSO₄, and filtered, and the solvent was removed under vacuum on a rotary evaporator. The resulting material was purified by chromatography on a Florisil column eluted with a 4:1 mixture of CH₂Cl₂ and ethyl acetate, and the mixed solvent was removed under vacuum. The solid was dissolved in a minimal amount of CH₂Cl₂, diethyl ether was layered over the solution, and the vessel stoppered and set aside in subdued light. Orange-red crystals were collected by filtration, washed with diethyl ether, and briefly air-dried to afford 0.970 g of (4-*t*-BuPy)Co(DH)₂SnPh₃·Et₂O (1.14 mmol), a 60% yield based on the limiting chlorotriphenyltin.

(4-*t*-Butylpyridine)triphenylleadcoloxime, (4-*t*-BuPy)Co(DH)₂PbPh₃. The compound was prepared by a procedure analogous to that above. (4-*t*-BuPy)Co(DH)₂Cl (0.90 g, 1.9 mmol) was reacted with 0.45 mL of 4.4 M NaOH and 0.070 g of NaBH₄ (1.9 mmol) to afford the cob(I)aloxime, which was reacted with 0.90 g of chlorotriphenyllead (1.7 mmol based on 90% purity). The Florisil column was eluted with CH₂Cl₂. Recrystallization by layering diethyl ether above CH₂Cl₂ afforded 0.68 g of red crystals of (4-*t*-BuPy)Co(DH)₂PbPh₃ (0.79 mmol), a 46% yield based on chlorotriphenyllead.

Description of X-ray Structural Analyses. Crystals were washed with the perfluoropolyether PFO-XR75 (Lancaster) and sealed under nitrogen in a glass capillary. The sample was optically aligned on the four-circle of a Siemens P4 diffractometer equipped with a graphite monochromator, a Mo K α radiation source ($\lambda = 0.71073$ Å), and a SMART CCD detector held at 5.054 cm from the crystal (5.084 cm for Co(DH)₂(NC₅H₄-*t*-Bu)). Four sets of 20 frames each were collected using the ω scan method and with a 10 s exposure time. Integration of these frames followed by reflection indexing and least-squares refinement produced a crystal orientation matrix for the crystal lattice.

The program SMART (version 5.6)²³ was used for diffractometer control, frame scans, indexing, orientation matrix calculations, least-squares refinement of cell parameters, and the data collection. All 1650 crystallographic raw data frames collected were read by the

Table 1. Crystal Data and Structure Refinements for (4-*t*-BuPy)Co(DH)₂SnPh₃·OEt₂, (4-*t*-BuPy)Co(DH)₂PbPh₃, and (4-*t*-BuPy)Co(DH)₂

empirical formula	C ₃₉ H ₅₂ CoN ₅ O ₅ Sn	C ₃₅ H ₄₂ CoN ₅ O ₄ Pb	C ₁₇ H ₂₇ CoN ₅ O ₄
fw, amu	848.48	862.86	424.37
<i>T</i> , K	295(2)	295(2)	295(2)
λ , Å	0.71073	0.71073	0.71073
space group	<i>P</i> 2 ₁ / <i>c</i>	<i>P</i> 2 ₁ / <i>n</i>	<i>Pbcn</i>
<i>a</i> , Å	11.6443(6)	15.0104(7)	17.9821(11)
<i>b</i> , Å	15.6085(8)	15.7693(8)	9.7449(6)
<i>c</i> , Å	22.6354(12)	16.6230(8)	22.7374(15)
α , deg	90	90	90
β , deg	96.634(1)	114.348(1)	90
γ , deg	90	90	90
<i>V</i> , Å ³	4086.4(4)	3584.8(3)	3984.4(4)
<i>Z</i>	4	4	8
ρ_{calcd} , g/cm ³	1.379	1.599	1.415
μ , cm ⁻¹	10.63	51.96	8.94
final <i>R</i> indices	<i>R</i> 1 = 0.0305	<i>R</i> 1 = 0.0251	<i>R</i> 1 = 0.0430
[<i>I</i> > 2 σ (<i>I</i>)]	w <i>R</i> 2 = 0.0725	w <i>R</i> 2 = 0.0549	w <i>R</i> 2 = 0.1099
<i>R</i> indices	<i>R</i> 1 = 0.0420	<i>R</i> 1 = 0.0358	<i>R</i> 1 = 0.0579
(all data)	w <i>R</i> 2 = 0.0772	w <i>R</i> 2 = 0.0582	w <i>R</i> 2 = 0.1230

program SAINT (version 5/6.0) and integrated using 3D profiling algorithms. The resulting data were reduced to produce the intensities and estimated standard deviations of reflections. An absorption correction was applied using the SADABS routine available in SAINT. The data were corrected for Lorentz and polarization effects. No evidence of decomposition was observed during any of the three data collections. Data preparation was carried out by using the program XPREP.

Structures were solved by use of SHELXTL 6.1.²⁴ Idealized positions for most of the hydrogen atoms were included as fixed contributions using a riding model with isotropic temperature factors set at 1.2 (aromatic and methylene protons) or 1.5 (methyl protons) times that of the adjacent carbon atom. The positions of the methyl hydrogen atoms were optimized by a rigid rotating group refinement with idealized tetrahedral angles. The positions of the two O–H protons of the dimethylglyoxime ligands were refined isotropically. Full-matrix least-squares refinement was based upon the minimization of $\sum w_i |F_o^2 - F_c^2|^2$, with weighting w_i^{-1} appropriate for each structure (see below). Final discrepancy indices and goodness of fit (GOF) values were calculated as $R1 = \sum(|F_o| - |F_c|)/\sum|F_o|$, $wR2 = [\sum[w(F_o^2 - F_c^2)^2]/\sum[w(F_o^2)^2]]^{1/2}$, $R_{\text{int}} = \sum|F_o^2 - F_o^2(\text{mean})|^2/\sum|F_o^2|$, and $\text{GOF} = [\sum[w(F_o^2 - F_c^2)^2]/(n - p)]^{1/2}$, where *n* is the number of reflections and *p* is the total number of parameters that were varied during the last refinement cycle.

A correction for secondary extinction was not applied. The linear absorption coefficient, atomic scattering factors, and anomalous dispersion corrections were calculated from values found in the International Tables of X-ray Crystallography.²⁵

Details specific to each of the three individual structures are described below. The refined lattice parameters and other pertinent crystallographic information for the three structures are summarized in Table 1. CCDC 649238–649240 contain the supplementary crystallographic data for (4-*t*-BuPy)Co(DH)₂X, where X = SnPh₃, PbPh₃, no ligand, respectively. These data can be obtained free of charge from the Cambridge Crystallographic Data Centre via www.ccdc.cam.ac.uk/data_request/cif.

(24) Sheldrick, G. M. *SHELXTL6.1, Crystallographic software package*; Bruker AXS, Inc.: Madison, WI, 2000.

(25) International Tables for X-ray Crystallography; Kynoch Press: Birmingham (Present distributor, D. Reidel, Dordrecht), 1974; Vol. IV, p 55.

(23) SMART, SAINT, and XPREP programs are part of the Bruker crystallographic software package for single crystal data collection, reduction, and preparation.

(4-*t*-BuPy)Co(DH)₂SnPh₃·OEt₂. Data reduction produced a total of 28 554 reflections, and preparation gave 9291 unique reflections ($R_{\text{int}} = 3.25\%$) with indices $-13 \leq h \leq 15$, $-20 \leq k \leq 20$, $-29 \leq l \leq 29$. The monoclinic space group was determined to be $P2_1/c$ (No. 14).

The structure was solved by a combination of the Patterson method and difference Fourier analysis. The crystallographic asymmetric unit also contains a molecule of ether. The three methyl groups of the *t*-butyl substituent suffer from a ca. 60:40 two-site disorder. During the final stages of refinement, the pairs of C–O and C–C bond distances within the ether molecule and the six pairs of C–C(Me) bonds within the disordered *t*-butyl substituent were restrained by the SADI command with esd's of ± 0.04 , ± 0.04 , and ± 0.02 Å, respectively. Full-matrix least-squares refinement, based upon the minimization of $\sum w_i |F_o^2 - F_c^2|^2$, with weighting $w_i^{-1} = [\sigma^2(F_o^2) + (0.0353P)^2 + 0.63P]$, where $P = (\max(F_o^2, 0) + 2F_c^2)/3$, converged to give final discrepancy indices of $R1 = 0.0305$, $wR2 = 0.0725$ for 7586 data with $I > 2\sigma(I)$. The GOF value was 1.026. The maximum and minimum residual electron density peaks in the final difference Fourier map were 0.406 and -0.260 e/Å³, respectively.

(4-*t*-BuPy)Co(DH)₂PbPh₃. Data reduction produced a total of 25 077 reflections, and preparation gave 8169 unique reflections ($R_{\text{int}} = 3.19\%$) with indices $-19 \leq h \leq 18$, $-20 \leq k \leq 20$, $-21 \leq l \leq 21$. The monoclinic space group was determined to be $P2_1/n$, a nonstandard setting of $P2_1/c$ (No. 14).

The structure was solved by a combination of the direct methods and difference Fourier analysis. The three methyl groups of the *t*-butyl substituent suffer from a ca. 60:40 two-site disorder, which was refined with the six C–C bonds restrained to 1.54 ± 0.02 Å. Full-matrix least-squares refinement, based upon the minimization of $\sum w_i |F_o^2 - F_c^2|^2$, with weighting $w_i^{-1} = [\sigma^2(F_o^2) + (0.0243P)^2 + 0.0993P]$, where $P = (\max(F_o^2, 0) + 2F_c^2)/3$, converged to give final discrepancy indices of $R1 = 0.0251$, $wR2 = 0.0549$ for 6663 data with $I > 2\sigma(I)$. The GOF value was 1.014. The maximum and minimum residual electron density peaks in the final difference Fourier map were 0.566 and -0.366 e/Å³, respectively.

(4-*t*-BuPy)Co(DH)₂. Data reduction produced a total of 24 743 reflections, and preparation gave 4557 unique reflections ($R_{\text{int}} = 6.27\%$) with indices $-23 \leq h \leq 23$, $-11 \leq k \leq 12$, $-29 \leq l \leq 29$. The orthorhombic space group was determined to be $Pbcn$ (No. 60).

The structure was solved by a combination of the direct methods and difference Fourier analysis. Carbon atoms C(9), C(10), C(12), and C(13) suffer from a two-site ca. 90:10 disorder which was refined by restraining the two C–N and four C–C distances within the minor site of the pyridine ring at 1.35 ± 0.02 and 1.39 ± 0.02 Å, respectively. Full-matrix least-squares refinement, based upon the minimization of $\sum w_i |F_o^2 - F_c^2|^2$, with weighting $w_i^{-1} = [\sigma^2(F_o^2) + (0.0612P)^2 + 0.84P]$, where $P = (\max(F_o^2, 0) + 2F_c^2)/3$, converged to give final discrepancy indices of $R1 = 0.0430$, $wR2 = 0.1099$ for 3560 data with $I > 2\sigma(I)$. The GOF value was 1.035. The maximum and minimum residual electron density peaks in the final difference Fourier map were 0.254 and -0.674 e/Å³, respectively.

Results

Syntheses of Complexes. The starting material (4-*t*-BuPy)Co(DH)₂Cl was prepared in a two-step procedure that involved ligand substitution of an axial base for a chloride ligand in Co(DH)(DH₂)Cl₂.²¹ This approach is more general than the original one-step preparation of cobaloxime com-

pounds,²⁶ which can afford significant amounts of [Co(DH)₂L₂][Co(DH)₂Cl₂] salt impurities for certain L.²¹

We employed 4-*tert*-butylpyridine as the axial base instead of pyridine, the more commonly used base in cobaloxime chemistry. The importance of the use of *tert*-butylpyridine for improved solubility properties and simplified ¹H NMR spectra is well documented.^{27–29} Substitution of 4-*tert*-butylpyridine for pyridine also slows the rate(s) of exchange processes in cobaloximes. Our observations show that the line width of the resonance for the hydrogen-bonded protons that link the two anionic dimethylglyoximate ligands narrows enough that the resonance can be observed for cobaloxime complexes containing most anionic, axial ligands. Moreover, exchange of these protons and of axial ligands between cobaloxime complexes with different axial ligands is sufficiently slow on the NMR time scale that individual resonances can be observed in mixtures.

(Py)Co(DH)₂EPh₃ complexes were synthesized by reaction of the strongly nucleophilic cob(I)aloxime with Ph₃EX compounds.^{18,19} Schrauzer used large molar excesses of NaBH₄ or Na/K alloy to reduce the starting cob(III)aloxime complex to cobalt(I).¹⁸ In the specific case of (Py)Co(DH)₂SnPh₃, both dropwise addition of a methanolic solution of Ph₃SnCl to the cob(I)aloxime in methanol and in situ reduction of (Py)Co(DH)₂Cl in the presence of Ph₃SnCl afforded product in good yield. Triphenyltin acetate, hydroxide, and hydride were also used successfully.¹⁸ The product precipitated rapidly upon mixing of the electrophile and cob(I)aloxime. The germanium, lead, and silicon analogues were prepared by slow addition of an ethereal solution of Ph₃EX to cob(I)aloxime in methanol. In all cases, the product was collected by filtration, washed, and purified by recrystallization. Tada's preparation of (4-*t*-BuPy)Co(DH)₂SnPh₃ incorporated several modifications.¹⁹ Addition of an equivalent of aqueous NaOH permitted the amount of NaBH₄ used to reduce the starting cobaloxime to be decreased to a slight molar excess. Chlorotriphenyltin was added as a solid. Finally, the product was extracted from the reaction mixture and purified by chromatography and recrystallization.

Synthesis of (4-*t*-BuPy)Co(DH)₂SnPh₃ proceeded in our hands much as reported. The slow formation and precipitation of product that we noted contrasts with Schrauzer's observations. This may reflect the lower reaction temperature that we employed. Initially, we conducted the extraction and chromatographic purification of the product under a nitrogen atmosphere. However, the product has sufficient air stability that this precaution is unnecessary. Collection of the initial precipitate by filtration followed by recrystallization also affords reasonably pure product. Our recrystallized product differed from that of Tada¹⁹ by including one ethyl ether molecule of solvation per complex. This disparity probably

(26) Schrauzer, G. N. *Inorg. Synth.* **1968**, *11*, 61–70.

(27) Bulkowski, J.; Cutler, A.; Dolphin, D.; Silverman, R. B. *Inorg. Synth.* **1980**, *20*, 127–134.

(28) Gupta, B. D.; Yamuna, R.; Singh, V.; Tiwari, U. *Organometallics* **2003**, *22*, 226–232.

(29) Chadha, P.; Gupta, B. D.; Mahata, K. *Organometallics* **2006**, *25*, 92–98.

results from differences in recrystallization technique or subsequent handling. Layering ether over CH_2Cl_2 likely leads to a higher ether concentration in solution when crystallization occurs than does vapor diffusion of ether. Crystals of $(4-t\text{-BuPy})\text{Co}(\text{DH})_2\text{SnPh}_3 \cdot \text{OEt}_2$ readily lose ether on standing at room temperature. The translucent orange-red crystals develop a powdery, opaque yellow-brown surface layer. Crystals stored in a small, tightly stoppered container change appearance slowly. Nonetheless, a strong odor of ether is evident when the container is opened. The NMR and structural properties of the complex are presented below.

The synthesis of $(4-t\text{-BuPy})\text{Co}(\text{DH})_2\text{PbPh}_3$ was carried out and occurred in a manner similar to that of the corresponding tin complex. Solid Ph_3PbCl reacted slowly with the cob(I)-aloxime at 0°C . We did not have to exercise any special caution to prevent an overly vigorous reaction and the formation of elemental lead.¹⁸ Ph_3PbCl is a technical grade material. Thus, chromatographic purification of the lead complex serves more of a purpose than in the case of tin. The lead complex appears to be less tightly held by the column and elutes well without addition of ethyl acetate to the methylene chloride. Like the tin complex, the lead complex has sufficient air stability to permit aerobic chromatography and recrystallization. No solvent molecules are included in the lattice. The NMR spectra and structure of $(4-t\text{-BuPy})\text{Co}(\text{DH})_2\text{PbPh}_3$, below, closely resemble those of the tin complex.

We were unable to prepare the germanium and silicon complexes $(4-t\text{-BuPy})\text{Co}(\text{DH})_2\text{GePh}_3$ and $(4-t\text{-BuPy})\text{Co}(\text{DH})_2\text{SiPh}_3$. If the complexes did form during the reactions that we attempted, they are significantly more labile than the analogous tin or lead complexes. The desired compounds were still not isolated when the level of caution in handling was increased from performing the workup aerobically to employing full Schlenk and finally drybox techniques. One major problem was the limited solubility of triphenylchlorogermane in methanol and other solvents. Substantial amounts of Ph_3GeCl were recovered unchanged when it was added as a solid to a solution of cob(I)aloxime in methanol. In an effort to find conditions in which Ph_3GeCl was dissolved and available in the reaction solution, we examined the reaction in several solvents.

Schrauzer reported preparing $(\text{Py})\text{Co}(\text{DH})_2\text{GePh}_3$ by reacting a solution of 5 mmol of $(\text{Py})\text{Co}(\text{DH})_2^-$ in 20 mL of methanol with a solution of 5 mmol of Ph_3GeCl in 5 mL of diethyl ether. A brown crystalline product was collected by filtration, washed with deoxygenated methanol, and recrystallized. We could not reproduce these observations. Roughly 20 mL of diethyl ether were required to dissolve 5 mmol of Ph_3GeCl . Reaction of this solution with $(4-t\text{-BuPy})\text{Co}(\text{DH})_2^-$ did afford a brown precipitate, but only after several days. Unexpectedly, the solid redissolved in methanol when washed after filtration. The ^1H NMR spectrum of the residue recovered from the combined filtrate and methanol wash established that it was a mixture of triphenylgermanium hydride (phenyl multiplet at 7.5 ppm and hydride singlet at

5.65 ppm^{30,31}); two cob(III)aloxime complexes with unknown anionic ligands (shown by presence of two distinct peaks for bridging O—H—O groups); and a paramagnetic, presumably cobalt(II) complex (broad peaks at -3.7 , 29.6 , 37.3 , 60 , and 80 ppm).

Triphenylchlorogermane is relatively soluble in THF. Hence, we attempted the synthesis in both mixed THF/methanol and THF solution. Addition of a solution of 5 mmol of Ph_3GeCl in 4 mL of THF to an equivalent amount of $(4-t\text{-BuPy})\text{Co}(\text{DH})_2^-$ in 20 mL of methanol resulted in a color change from blue to brown, but no product precipitated. Evaporation of the solution afforded a residue that was initially soluble in CDCl_3 . Within minutes, a precipitate began to form. The ^1H NMR spectrum of the residue showed that it was at best grossly impure. It had broad lines at chemical shift regions near those expected for $(4-t\text{-BuPy})\text{Co}(\text{DH})_2\text{GePh}_3$, but multiple peaks were observed in the dimethylglyoximate methyl and pyridine *tert*-butyl group regions. Attempts to purify the residue by chromatography afforded a material whose ^1H NMR spectrum established that it contained the $(4-t\text{-BuPy})\text{Co}^{\text{III}}(\text{DH})_2$ moiety but lacked any phenyl groups. In contrast to these results, reaction of Ph_3GeCl with $(4-t\text{-BuPy})\text{Co}(\text{DH})_2^-$ in THF produced a substantial amount of a brown crystalline product. X-ray crystallography (see below) established that the solid was the cobalt(II) complex $(4-t\text{-BuPy})\text{Co}(\text{DH})_2$. The filtrate from this reaction contained triphenylgermanium hydride and a paramagnetic complex. Thus, $(4-t\text{-BuPy})\text{Co}(\text{DH})_2\text{GePh}_3$ is either unstable under these reaction conditions or is not formed.

Reaction of an ethereal solution of Ph_3SiCl with $(4-t\text{-BuPy})\text{Co}(\text{DH})_2^-$ in methanol failed to produce $(4-t\text{-BuPy})\text{Co}(\text{DH})_2\text{SiPh}_3$. The brown solid that precipitated was only slightly soluble in chloroform or DMSO and insoluble in most other solvents. The ^1H NMR spectrum of this solid in CDCl_3 showed that it was not a cobaloxime compound. In addition, the expected cobaloxime complex was not detected in the NMR spectrum of the residue recovered from the filtrate.

Finally, we re-examined the syntheses of trichlorotin cobaloxime complexes. Schrauzer reported that reaction of $\text{SnCl}_2 \cdot 2\text{H}_2\text{O}$ with $\text{LCo}(\text{DH})_2\text{Cl}$ in methanol affords a poorly soluble $\text{LCo}(\text{DH})_2\text{SnCl}_3$ complex when $\text{L} = \text{pyridine}$ or *aniline*.²⁶ The *aniline*-containing complex was recrystallized from a 1:1 mixture of HCl containing methanol and water. A similar approach was used to prepare trichlorotin—rhodium tetraphenylporphyrin, $\text{Rh}(\text{TPP})-\text{SnCl}_3$.³² Reaction of $\text{SnCl}_2 \cdot 2\text{H}_2\text{O}$ with $(4-t\text{-BuPy})\text{Co}(\text{DH})_2\text{Cl}$ produced a brown solid that was nearly completely insoluble in every solvent that we examined. It was not readily recrystallized from a mixture of acidic methanol and water. Only a small fraction of the mass of the material dissolved in the boiling mixed solvent or in boiling dilute HCl , which was subsequently diluted with

(30) Clark, K. B.; Griller, D. *Organometallics* **1991**, *10*, 746–750.

(31) Woo, H.-G.; Freeman, W. P.; Tilley, T. D. *Organometallics* **1992**, *11*, 2198–2205.

(32) Licocchia, S.; Paolesse, R.; Boschi, T.; Bandoli, G.; Dolmella, A. *Acta Crystallogr.* **1995**, *C51*, 833–835.

Table 2. ^1H NMR Data for Cobaloxime Compounds (4-*t*-BuPy)Co(DH) $_2$ X^a

X	solvent	CH $_3$ ^b	O–H–O ^c	<i>t</i> -Bu ^d	α -H ^e	β -H ^e	X
Cl	CDCl $_3$	2.38	~18.2	1.21	8.06	7.15	
	C $_6$ D $_6$	1.89	19.49	0.52	8.45	6.26	
<i>n</i> -Bu	CDCl $_3$	2.13	18.25	1.27	8.43	7.26	0.80 ^f , 0.88 ^g , 1.20 ^h , 1.61 ⁱ
SnPh $_3$	CDCl $_3$ ^j	1.73	18.56	1.25	8.41 ^k	7.27 ^l	7.51 ^m , 7.26 ⁿ , 7.28 ^o
	C $_6$ D $_6$ ^p	1.58	19.63	0.64	8.84	6.53	7.90 ^q , 7.1–7.2 ^r
PbPh $_3$	CDCl $_3$	1.79 ^s	18.65	1.24	8.36 ^t	7.25 ^u	7.44 ^v , 7.28 ^w , 7.21 ^x
	C $_6$ D $_6$	1.65 ^s	19.76	0.63	8.79 ^y	6.51	7.86 ^v , 7.22 ^w , 7.09 ^x

^a ppm relative to TMS at 21 °C. ^b s, 12 H. ^c br s, 2 H. ^d s, 9H. ^e AA'BB', ³ $J_{\alpha\beta}$ = 6.0, Hz, 2H. ^f δ -C, t, 3H. ^g β -C, m, 2H. ^h γ -C, m, 2H. ⁱ α -C, diastereotopic m, 2H. ^j Ether of solvation: 1.20 (t, 6H), 3.47 (q, 4H). ^k ³ J_{SnH} = 10.2 Hz. ^l Overlaps phenyl *m,p*-H multiplet, 2H. ^m m, 6H, *o*-H, ³ J_{SnH} = 40.2 Hz. ⁿ m, 6H, *m*-H. ^o m, 3H, *p*-H. ^p Ether of solvation: 1.13 (t, 6H), 3.26 (q, 4H). ^q dd, J_{HH} = 7.0, 1.6 Hz, 6H, *o*-H, ³ J_{SnH} = 40.0 Hz. ^r m, 9H, *m,p*-H. ^s long range J_{PbH} = 6.4 Hz. ^t ⁴ J_{PbH} = 19.0 Hz. ^u Overlaps phenyl *m,p*-H multiplet, 2H. ^v dd, J_{HH} = 7.0, 1.6 Hz, 6H, *o*-H, ³ J_{PbH} = 52.8 Hz.

an equal volume of methanol to affect crystallization. Orange crystals formed on standing at room temperature, but the recrystallization had a strong odor of 2,3-butanedione from hydrolysis of the dimethylglyoxime ligand. It is quite unlikely that the brown solid is a mononuclear complex containing a bond between Co and the Sn of an axial trichlorotin ligand as implied in the original report. Rather, it is probably an oligomeric material in which Sn bridges the oxygens of dimethylglyoximate ligands coordinated to different cobalt ions. IR data support this conjecture. Schrauzer reported that the SnCl $_3$ complex has an N–O stretching frequency of 1217 cm $^{-1}$, which is identical within error with the IR spectrum of the material that we obtained. In contrast, mononuclear, Co–Sn-bonded LCo(DH) $_2$ –SnR $_3$ complexes have N–O stretching frequencies that are 15–30 cm $^{-1}$ higher.

NMR Spectroscopy. ^1H chemical shift data for the triphenylstannyl- and triphenylplumbylcobaloxime complexes (4-*t*-BuPy)Co(DH) $_2$ X (X = SnPh $_3$ and PbPh $_3$) in both CDCl $_3$ and C $_6$ D $_6$ solution are reported in Table 2. ^{13}C chemical shift data in CDCl $_3$ are reported in Table 3.

The ^1H spectral data for (4-*t*-BuPy)Co(DH) $_2$ SnPh $_3$ in CDCl $_3$ solution are mostly consistent with that obtained by Tada at 90 MHz. Exceptions include the extra peaks observed for the diethyl ether of solvation and the much narrower chemical shift range of the phenyl proton peaks of the Ph $_3$ -Sn group. The latter are the most notable feature of the spectrum. The ortho proton multiplet resembles an incompletely resolved doublet of a triplet. Additionally, it has satellites due to coupling to the two spin 1/2 isotopes ^{117}Sn and ^{119}Sn , which are, respectively, 7.61% and 8.58% abundant. The ³ J_{SnH} coupling constant of 40.2 Hz for this complex is slightly smaller than the 43.7 Hz coupling in Co(OEP)SnPh $_3$.¹ The poorly resolved meta and para proton multiplet overlaps and obscures the multiplet for the β -proton of the 4-*t*-BuPy axial base. The corresponding multiplet for the α -proton is part of a distinctive AA'BB' second-order pattern. Selective decoupling of the β -proton multiplet collapses the α -proton multiplet to reveal a 10.2 Hz coupling of the α -proton to Sn. Simulations of these multiplets in this

and the other complexes establish that the AB coupling constants are about 6.0 Hz, the BB' couplings ranges from 1.6 to 2.3 Hz, the AB' from 0.7 to 1.1 Hz, and the AA' from 0.1 to 0.6 Hz.

Most of the ^{13}C resonances of (4-*t*-BuPy)Co(DH) $_2$ SnPh $_3$ are readily assigned on the basis of their chemical shifts and comparisons to literature data for pyridine and 4-*t*-BuPy cobaloxime complexes.^{28,33,34} Exceptions include the dimethylglyoximate imine (C=N) and the 4-*t*-BuPy C $_{\alpha}$ carbons, which have similar chemical shifts, and the phenyl carbons of the triphenyltin group. The assignments of these carbons were verified by APT and HETCOR experiments. All four phenyl carbons exhibit coupling to the Sn.

Although the ^1H and ^{13}C spectra of (4-*t*-BuPy)Co(DH) $_2$ PbPh $_3$ in CDCl $_3$ closely resemble those of the analogous tin complex, there are significant differences. The methyl proton peak of the equatorial dimethylglyoximate ligands shifts downfield, and the axial 4-*t*-BuPy and Ph $_3$ Pb proton peaks shift upfield slightly relative to the corresponding peaks in the tin complex. In the ^{13}C spectrum, the shifts of the C=N, phenyl C $_{\text{meta}}$, and C $_{\text{ipso}}$ carbons increase by 0.5, 0.8, and 13.3 ppm, respectively, and the C $_{\text{para}}$ decreases by 0.5 ppm. The changes in C $_{\text{meta}}$ and C $_{\text{para}}$ shifts invert the order of their resonances. Other differences include the increased resolution of the peaks in the phenyl proton multiplets and the greater extent of coupling to lead. The ortho proton multiplet resembles a doublet of a doublet, and the meta and para proton multiplet has several well-resolved components. The coupling constant of the ortho proton peak to the 22.6% abundant, spin 1/2 ^{207}Pb isotope is 52.8 Hz, and that of the α -proton of 4-*t*-BuPy is 19.0 Hz. Unlike tin, long-range coupling of the lead isotope to the methyl protons and carbons of the dimethylglyoximate ligands and C $_{\alpha}$ and C $_{\beta}$ is observed.

The ^1H spectra of the tin and lead complexes are extremely sensitive to solvent. Very large changes in the chemical shifts are observed in C $_6$ D $_6$ solution. The direction and size of the change varies for different protons in the complex in a manner that would seem unusual for simple solvation changes. The peak for the hydrogen-bonded protons (O–H–O) that link the two anionic dimethylglyoximate ligands shift downfield by nearly 1.1 ppm. The pyridine α -proton and Ph $_3$ E ortho proton peaks shift downfield by about 0.4 ppm. In contrast, the pyridine β -proton peak shifts upfield by 0.7 ppm, which is more than sufficient to make it well separated from the meta and para phenyl multiplet. The pyridine *t*-butyl protons shift upfield by 0.6 ppm. The remaining protons have smaller upfield shifts. Another striking change is a simplification of the appearance of the phenyl proton multiplets. The ortho proton peaks of both the lead and tin complexes are simple doublets of doublets. And the meta and para proton multiplets are better resolved and simpler in appearance.

The marked change in the complexity of the phenyl proton multiplets and their wide chemical shift range at 90 MHz

(33) Bied-Charreton, C.; Septe, B.; Gaudemer, A. *Org. Mag. Reson.* **1975**, *7*, 116–124.

(34) Stewart, R. C.; Marzilli, L. G. *Inorg. Chem.* **1977**, *16*, 424–427.

Table 3. ^{13}C NMR Data for Cobaloxime Compounds (*4-t*-BuPy)Co(DH) $_2$ X^a

X	DH		<i>t</i> -BuPy					X			
	CH ₃	C=N	C _α	C _β	C _γ	C _q	CH ₃	C _α	C _β	C _γ	C _δ
Cl	13.2	152.5	150.3	123.1	163.8	35.1	30.1				
<i>n</i> -Bu	12.0	148.8	149.4	122.3	161.6	34.8	30.2	C _α 32.1 ^b	C _β 32.9	C _γ 23.7	C _δ 13.9
SnPh ₃	11.9	150.5	148.5	122.6	161.6	34.8	30.2	C _{ipso} 141.1 ^c	C _{ortho} 137.1 ^d	C _{meta} 127.5 ^e	C _{para} 128.0 ^f
PbPh ₃	11.9 ^g	151.0 ^h	148.7 ⁱ	122.8 ^j	161.7	34.8	30.2	154.4 ^k	137.1 ^l	128.3 ^m	127.5 ⁿ

^a ppm relative to TMS in CDCl₃ at 21 °C. ^b Line width (fwhh) = 35 Hz at 50 °C. ^c $^1J(^{119}\text{Sn}, \text{C}_{\text{ipso}}) = 314.8$ Hz, $^1J(^{117}\text{Sn}, \text{C}_{\text{ipso}}) = 300.5$ Hz. ^d $^2J(\text{Sn}, \text{C}_{\text{ortho}}) = 32.3$ Hz. ^e $^3J(\text{Sn}, \text{C}_{\text{meta}}) = 42.3$ Hz. ^f $^4J(\text{Sn}, \text{C}_{\text{para}}) = 11.2$ Hz. ^g $^3J(\text{Pb}, \text{C}) = 6.2$ Hz. ^h $^2J(\text{Pb}, \text{C}) = 9.5$ Hz. ⁱ $^2J(\text{Pb}, \text{C}_{\alpha}) = 7.5$ Hz. ^j $^3J(\text{Pb}, \text{C}_{\beta}) = 18.2$ Hz. ^k $^1J(\text{Pb}, \text{C}_{\text{ipso}}) = 60.2$ Hz. ^l $^2J(\text{Pb}, \text{C}_{\text{ortho}}) = 32.3$ Hz. ^m $^3J(\text{Pb}, \text{C}_{\text{meta}}) = 46.5$ Hz. ⁿ $^4J(\text{Pb}, \text{C}_{\text{para}}) = 14.8$ Hz.

may reflect dynamic processes in the Ph₃E groups. If rotation of the Ph₃E phenyl groups in CDCl₃ is slow, especially for the tin complex, exchange of ortho and meta protons between environments inside and outside the Ph₃E cone would be slow. Complicated multiplets will be observed. Faster rotation on the NMR time scale in C₆D₆ solution would result in fast exchange, averaging of environments, and simpler spectra.

The chemical shift data for (*4-t*-BuPy)Co(DH) $_2$ X with X = SnPh₃ and PbPh₃ show a much closer correspondence of the pyridine proton shifts with those of the alkylcobaloxime (X = *n*-Bu) than the chlorocobaloxime (X = Cl), Table 2. Investigations of the NMR of LCo(DH) $_2$ X complexes reveal a correlation between the pyridine α -H shift and the position of X in the spectrochemical series, which presumably arises from the effect of the ligand on mixing of a paramagnetic excited-state of cobalt(III) into the ground state.²¹ To a first approximation, then, the Ph₃Sn and Ph₃Pb ligands are similar to alkyl ligands in terms of donor strength and the covalency of the Co–X bond. The same authors noted a correlation between the pyridine α -proton and dimethylglyoximate methyl group chemical shifts.²¹ The X = *n*-Bu complex fits the correlation well. However, the dimethylglyoximate methyl group shifts of the tin and lead complexes are 0.40 and 0.34 ppm upfield of the predicted values. These deviations probably result from shielding of the methyl protons by the phenyl ring currents of the axial Ph₃E groups. The strong NOE observed in a NOESY spectrum between these methyl protons and both the ortho and meta Ph₃Sn phenyl protons is consistent with the phenyl ring orientation necessary for shielding.

Other workers have noted a correlation between the chemical shifts of the pyridine α -H, bridging O–H–O, and C=N carbon.^{35,36} In general, downfield shifts of the former two are accompanied by upfield shifts of the carbon. A field effect model that involves ring current in the glyoxime ligands in addition to cobalt anisotropy was advanced to explain the correlation.^{35,36} The correlation does not appear to hold in the current series of compounds. The shift of the bridging O–H–O proton increases in the order X = Cl < *n*-Bu < Ph₃Sn < Ph₃Pb. However, both the pyridine α -H and C=N carbon of the Sn and Pb complexes have shifts between those of the Cl and *n*-Bu complexes.

Several features of the NMR of the butylcobaloxime are noteworthy. The complete assignment of the butyl proton peaks by selective decoupling shows that the shifts do not increase monotonically as one moves from the methyl toward the cobalt (δ to α). The β -H has a shift close to that of the methyl group and is 0.32 ppm upfield of the γ -H. This anomaly does not appear to have been noted in the literature previously inasmuch as the shifts of the alkyl protons are typically reported as a range and not specifically assigned. The butyl C_α ^{13}C peak was not observed at room temperature, owing to its extremely broad line width. Warming to 50 °C narrowed the line to a 35 Hz width. Both of these features are reminiscent of the phenomena observed for alkyl cobalt(III)porphyrin complexes, which were ascribed to paramagnetic contact shifts that arise from thermal population of an excited-state of the quadrupolar cobalt.³⁷ Solvent effects on the anisotropy and the energy difference between the ground and excited states of cobalt might be responsible for the extreme sensitivity of the chemical shifts of the cobaloxime complexes to solvent.

Structures. ORTEP drawings of the independent molecules of (*4-t*-BuPy)Co(DH) $_2$ SnPh₃ and (*4-t*-BuPy)Co(DH) $_2$ PbPh₃ are presented in Figures 1 and 2, respectively. Figure 3 shows two related molecules of (*4-t*-BuPy)Co(DH) $_2$. Selected bond lengths and bond angles for the three structures are listed in Table 4.

The structure of (*4-t*-BuPy)Co(DH) $_2$ SnPh₃, Figure 1, has distorted octahedral coordination at cobalt and is similar to those of six-coordinate, alkylpyridine cobaloxime complexes.^{38–40} Bond distances and angles within the (DH) $_2$ unit are unremarkable.³⁸ The (DH) $_2$ unit is nearly planar. The 12 non-hydrogen atoms have a mean deviation of 0.042 Å, and the four nitrogen atoms have a mean deviation of 0.018 Å from the respective least-square planes that they define. Individual N_{eq}–Co–Sn angles range from 86.42(6)° to 90.91(6)°, whereas the N_{eq}–Co–N_{py} angles vary from 90.95(8)° to 92.28(8)°. As would be expected from these angles, the Co atom is displaced 0.055 Å from the plane defined by the four nitrogen atoms toward the axial *t*-BuPy ligand. This is the direction of displacement observed in most alkyl pyridine

(35) Gupta, B. D.; Yamuna, R.; Mandal, D. *Organometallics* **2006**, *25*, 706–714.

(36) Mandal, D.; Gupta, B. D. *Organometallics* **2005**, *24*, 1501–1510.

(37) Cao, Y.; Petersen, J. L.; Stolzenberg, A. M. *Inorg. Chim. Acta* **1997**, *263*, 139–148.

(38) Randaccio, L.; Bresciani-Pahor, N.; Zangrando, E.; Marzilli, L. G. *Chem. Soc. Rev.* **1989**, *18*, 225–250.

(39) Randaccio, L. *Comments Inorg. Chem.* **1999**, *21*, 327–376.

(40) Randaccio, L.; Furlan, M.; Geremia, S.; Slouf, M.; Srnova, I.; Toffoli, D. *Inorg. Chem.* **2000**, *39*, 3403–3413.

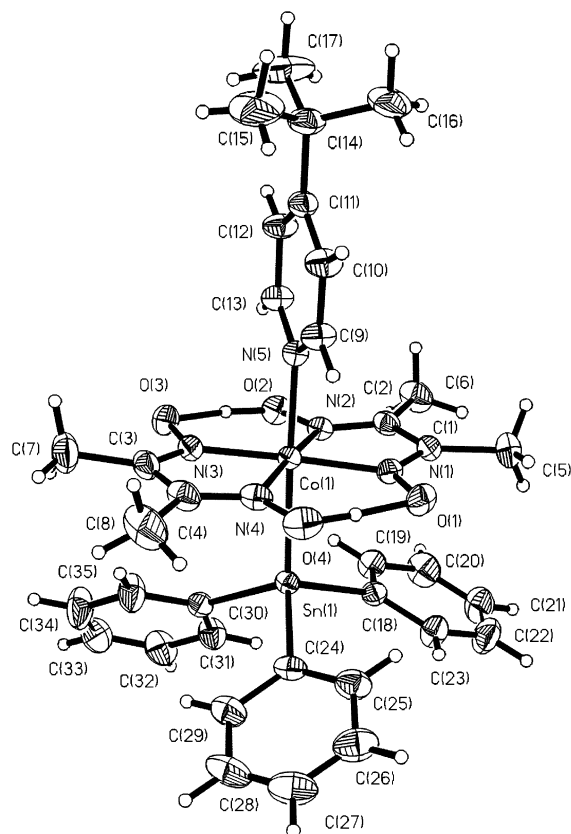


Figure 1. Perspective view of the molecular structure of (4-*t*-BuPy)Co(DH)₂SnPh₃ with the atom labeling scheme. The diethyl ether of solvation and the minor orientation of the disordered *t*-butyl group are not shown. Thermal ellipsoids are scaled to enclose 30% probability.

cobaloxime complexes.^{38,39,41} The N_{Py}–Co–Sn unit is slightly bent from linear with the Ph₃Sn group displaced toward N1 and N2.

The Co–L and Co–X bond lengths of LCo(DH)₂X are influenced by the σ -donor strength of the trans ligand and also by the steric bulk of the L and X groups.^{38,39} The Co–N_{Py} distances of 2.056(2) Å in (4-*t*-BuPy)Co(DH)₂SnPh₃ and 2.068(3) Å in (Py)Co(DH)₂CH₃⁴⁰ are quite similar. To the extent that the 4-*t*-butyl group does not affect the Co–N_{Py} distance, the Ph₃Sn and CH₃ groups would appear to have similar donor strengths.

There are few X-ray structures reported for complexes that contain a Co–SnPh₃ fragment. A search of the Cambridge Structural Database⁴² retrieved 14 structures, whose mean Sn–C_{ipso} distance is 2.175 Å and Co–Sn distances range from 2.489 to 2.598 Å and have a mean of 2.546(43) Å. Most of the longer Co–Sn distances occur in complexes that contain Co(I) in carbonyl or organometallic fragments. A 2.510(2) Å distance is found in five-coordinate Co(OEP)–SnPh₃,¹ where the cobalt is formally Co(III). This is significantly shorter than the 2.5568(3) Å Co–Sn distance in (4-*t*-BuPy)Co(DH)₂SnPh₃. The longer distance in the six-coordinate cobaloxime complex likely reflects the trans influence of the axial pyridine ligand. The magnitude of the

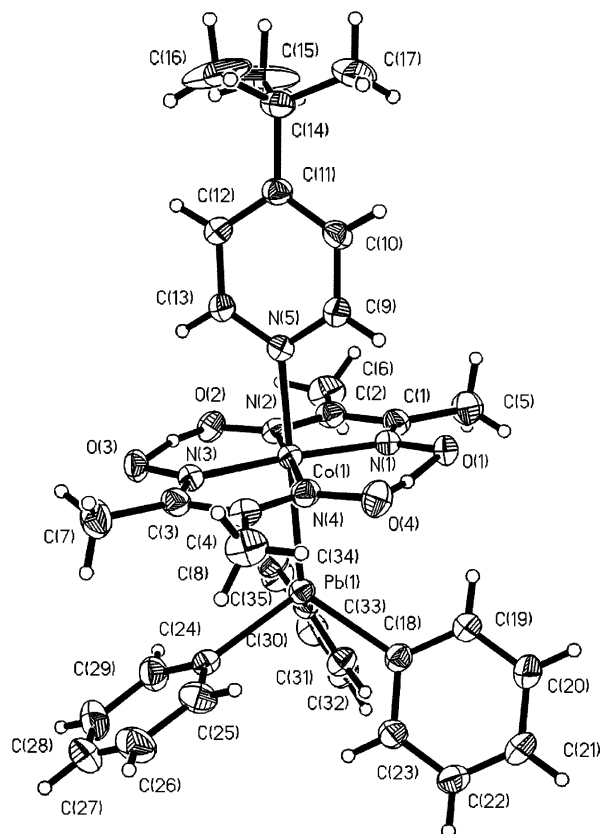


Figure 2. Perspective view of the molecular structure of (4-*t*-BuPy)Co(DH)₂PbPh₃ with the atom labeling scheme. The minor orientation of the disordered *t*-butyl group is not shown. Thermal ellipsoids are scaled to enclose 30% probability.

change in the Co–Sn distance is comparable to the difference in the Co–C distances in five-coordinate Co(OEP)CH₃ and six-coordinate PyCo(OEP)CH₃.⁴³

The Co–C _{α} –Y angles of alkyl pyridine cobaloxime complexes are larger than the 109.5° angle characteristic of an sp³-hybridized, tetrahedral carbon.^{38,41} Consequently, the contribution of the carbon s orbital to the hybrid orbital used in the Co–C bond is increased relative to an sp³ hybrid. A similar situation is found for the SnPh₃ groups, although the changes in the three Co–Sn–C_{ipso} angles are less than in the one or two Co–C–C angles present in alkyl cobaloximes. The values of these angles range from 109.89–(5)° to 116.37(6)° in (4-*t*-BuPy)Co(DH)₂SnPh₃ and 108.8(2)° to 121.1(2)° in Co(OEP)SnPh₃.¹ The mean value for the 14 examples in the database is 116(4)°.

(4-*t*-BuPy)Co(DH)₂PbPh₃, Figure 2, is nearly isostructural with the tin complex. Except for the absence of a solvent molecule in the asymmetric unit, the differences are subtle. The (DH)₂ unit of the Pb complex is more nearly planar. The 12 non-hydrogen atoms have a mean deviation of 0.017 Å, and the four nitrogen atoms have a mean deviation of 0.007 Å from the respective least-square planes that they define. The Co atom is displaced 0.073 Å from the plane defined by the four nitrogen atoms toward the axial *t*-BuPy ligand. The N_{Py}–Co–Pb unit is essentially linear. The Co–

(41) Randaccio, L.; Bresciani-Pahor, N.; Toscano, P. J.; Marzilli, L. G. *J. Am. Chem. Soc.* **1981**, *103*, 6347–6351.

(42) Allen, F. H. *Acta Crystallogr.* **2002**, *B58*, 380–388.

(43) Summers, J. S.; Petersen, J. L.; Stolzenberg, A. M. *J. Am. Chem. Soc.* **1994**, *116*, 7189–7195.

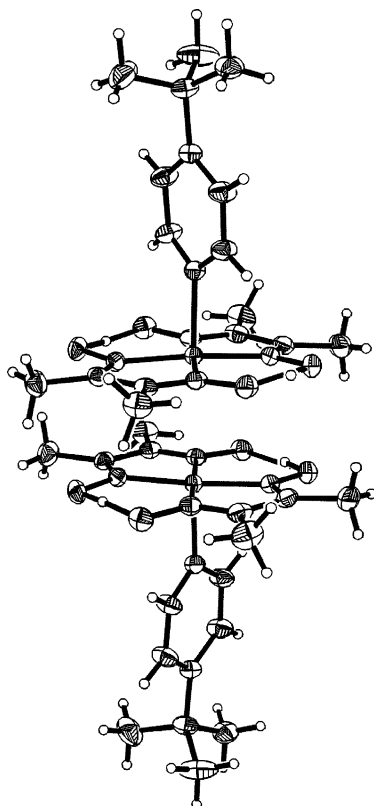


Figure 3. Perspective view of the dimeric units of (4-*t*-BuPy)Co(DH)₂ observed in the solid state. The Co–Co separation is 3.209 Å. The atom labeling scheme for the cobaloxime is the same as in Figure 1. The minor orientation of the disordered pyridine ring is not shown. The thermal ellipsoids are scaled to enclose 30% probability.

N_{py} distance of 2.049(2) Å is marginally shorter than the corresponding distance in the Sn complex, suggesting that the Ph₃Pb group is a comparable or at most a slightly weaker σ -donor than the Ph₃Sn group. All of the bond distances involving Pb are longer than the corresponding distances in the Sn complex, which is expected given the larger covalent radius of Pb compared to Sn. However, the increase is not uniform. The Co–Pb distance is 0.062 Å longer than the Co–Sn distance, but the average Pb–C_{ipso} distance is 0.091 Å longer than the average Sn–C_{ipso} distance. Interestingly, the Co–Pb–C_{ipso} angles are larger and the C_{ipso}–Pb–C_{ipso} angles smaller than the analogous angles in the Sn complex. Steric interactions between the Ph₃E group and the (DH)₂ unit cannot be responsible for the angular changes because the longer Co–Pb bond should reduce the severity of steric interactions. Apparently these changes reflect a difference in hybridization of Pb compared to Sn. The Pb *s* orbital contributes more to the Co–E bond than the Sn *s* orbital. Consequently, the Pb–C_{ipso} bonds have a greater Pb *p* orbital contribution and smaller C_{ipso}–Pb–C_{ipso} angles. Interestingly, the hybridization changes are consistent with the increased coupling of Pb to the equatorial DH and trans 4-*t*-BuPy ligands (compared to Sn) that is observed in the ¹H and ¹³C NMR spectra (vida supra).

There is only one report of an X-ray structure of a complex that contains a Co–PbPh₃ fragment.⁴⁴ The structure of this

Table 4. Selected Bond Lengths (Å) and Bond Angles (°) for (4-*t*-BuPy)Co(DH)₂X

	X		
	SnPh ₃ ^a	PbPh ₃	^b
Co–N(1)	1.8801(18)	1.880(3)	1.877(2)
Co–N(2)	1.8724(16)	1.875(3)	1.891(2)
Co–N(3)	1.8786(19)	1.881(2)	1.881(2)
Co–N(4)	1.8729(17)	1.880(3)	1.882(2)
Co–N(5) ^c	2.0564(18)	2.049(2)	2.096(2)
Co–E ^d	2.5568(3)	2.6191(4)	
Co–Co ^e			3.209
E–C(18)	2.151(2)	2.246(3)	
E–C(24)	2.155(2)	2.247(3)	
E–C(30)	2.156(2)	2.241(3)	
N(1)–Co–N(2)	81.46(8)	81.46(12)	81.56(8)
N(1)–Co–N(3)	177.70(8)	175.92(10)	175.10(7)
N(1)–Co–N(4)	98.44(9)	98.78(12)	98.44(8)
N(1)–Co–N(5)	91.34(8)	91.69(10)	92.40(7)
N(1)–Co–E	86.79(6)	88.42(7)	
N(2)–Co–N(3)	98.20(8)	98.17(11)	97.87(7)
N(2)–Co–N(4)	175.51(8)	175.10(10)	175.52(7)
N(2)–Co–N(5)	92.21(7)	91.76(10)	92.69(8)
N(2)–Co–E	86.42(6)	88.60(7)	
N(3)–Co–N(4)	81.71(9)	81.24(11)	81.75(7)
N(3)–Co–N(5)	90.95(8)	92.38(10)	92.49(7)
N(3)–Co–E	90.91(6)	87.51(7)	
N(4)–Co–N(5)	92.28(8)	93.12(10)	91.79(7)
N(4)–Co–E	89.10(6)	86.52(7)	
N(5)–Co–E	177.83(5)	179.63(8)	
Co–E–C(18)	109.89(5)	117.31(8)	
Co–E–C(24)	111.15(6)	112.69(7)	
Co–E–C(30)	116.37(6)	117.10(7)	
C(18)–E–C(24)	109.26(8)	102.68(11)	
C(18)–E–C(30)	103.62(8)	102.61(11)	
C(24)–E–C(30)	106.13(10)	102.38(11)	

^a Material also contains one diethyl ether molecule of solvation. ^b No axial ligand. ^c N(5) is pyridine nitrogen of 4-*t*-butylpyridine. ^d E = Sn or Pb. ^e Co' is cobalt in the second molecule of the solid-state dimer.

fragment in Ph₃PbCo(CO)₄ is not similar to that in (4-*t*-BuPy)Co(DH)₂PbPh₃. The Co–Pb distance of 2.667(2) Å in the carbonyl complex is 0.048 Å longer than in the cobaloxime. In contrast, the average Pb–C_{ipso} distance of 2.208 Å is 0.037 Å smaller. The C_{ipso}–Pb–C_{ipso} angles in the carbonyl complex are nearly tetrahedral. A total of 25 independent M–PbPh₃ fragments are found in the Cambridge Structural Database when the identity of the metal M is not restricted. The structures of the Ph₃Pb groups in these fragments are more closely related to that in (4-*t*-BuPy)Co(DH)₂PbPh₃. The mean Pb–C_{iso} distance is 2.230 Å, and the C_{ipso}–Pb–C_{ipso} angle is 104.1° in this population.

The X-ray structure of the cobalt-containing product isolated during attempts to prepare the Ph₃Ge complex established that it has composition (4-*t*-BuPy)Co(DH)₂, Figure 3. The structure of this complex is noteworthy in two respects. First, there are few structures reported for cob(II)-aloxime complexes. The two known examples are both of six-coordinate, octahedral complexes—Py₂Co(DH)₂⁴⁵ and a BF₂-linked cobaloxime (CH₃OH)₂Co(dmgBF₂)₂.⁴⁶ The Co–N_{eq} distances of 1.89 and 1.88 Å in these complexes are indistinguishable from that in cob(III)aloxime complexes, as is this distance in (4-*t*-BuPy)Co(DH)₂. In contrast, these low-

(45) Fallon, G. D.; Gatehouse, B. M. *Cryst. Struct. Commun.* **1978**, *7*, 263–267.

(46) Bakac, A.; Brynildson, M. E.; Espenson, J. H. *Inorg. Chem.* **1986**, *25*, 4108–4114.

(44) Geller, J. M.; Wosnick, J. H.; Butler, I. S.; Gilson, D. F. R.; Morin, F. G.; Bélanger-Gariépy, F. *Can. Chem. J.* **2002**, *80*, 813–820.

spin, d^7 complexes have two equivalent Co–axial ligand bond distances (Co–N_{Py} of 2.25 Å and Co–O of 2.264(4) Å) that are nearly 0.2 Å longer than Co–N_{Py} found in low-spin, d^6 cob(III)aloximes. Interestingly, the 2.096(2) Å Co–N_{Py} distance in (4-*t*-BuPy)Co(DH)₂ is much closer to the value in the six-coordinate cob(III)aloxime complexes.^{38–40} Another similarity is that the Co atom is displaced 0.077 Å from the plane of the four nitrogen atoms toward the axial pyridine ligand. Although the single electron in the metal–axial ligand σ -antibonding d_z^2 orbital increases the Co–N distance relative to cobalt(III) complexes, competition of two trans ligands for bonding to this orbital would appear to cause a more significant lengthening. The second remarkable feature of the structure is that (4-*t*-BuPy)Co(DH)₂ is not an isolated five-coordinate complex but rather is closely associated with a second molecule of the complex in the solid state. The two (4-*t*-BuPy)Co(DH)₂ units have CoN₄ planes that are inclined 1.4° from being parallel and are oriented so the oxygen-containing ‘rings’ of the two macrocycles are rotated roughly 90° with respect to each other. The N(2)–Co–N(4) vector of one unit nearly eclipses the N(4)–Co–N(2) vector of the second unit, i.e., the N(2)–Co–Co’–N(4)’ torsion is 4.2°. In this orientation the C(2)–N(2)–O(2) region in one unit eclipses the O(4)’–N(4)’–C(4)’ region in the second with C(2)–O(4)’, N(2)–N(4)’, and O(2)–C(4)’ contacts of 3.066, 3.065, and 3.161 Å, respectively. Given the unequal N–Co–N angles within the macrocycle, the N(1)–Co–Co’–N(3) torsion is larger (21.1°) and contacts in that region are larger. The Co–Co’ distance is 3.209 Å, which is 0.67 Å longer than the Co–Co single bond distance of 2.525 Å in Co₂(CO)₈.⁴⁷ Thus, the pairing of complexes in the lattice appears to result from weaker packing forces or ligand π – π interactions rather than stronger metal–metal bonding.

Magnetic Properties of [(4-*t*-BuPy)Co(DH)₂]. In the context of the pairing of complexes observed in the X-ray structure of [(4-*t*-BuPy)Co(DH)₂], it is worth noting that Schrauzer reported isolating dimeric, diamagnetic cob(II)-aloximes of composition [LCo(DH)₂]₂.⁴⁸ Halpern reported that materials that he obtained following Schrauzer’s procedure had paramagnetic moments in the range expected for a low-spin d^7 complex.⁴⁹ He concluded that the complexes were monomeric, both in their solid forms and in solution.

Magnetic susceptibility measurements on a bulk sample of [(4-*t*-BuPy)Co(DH)₂] from the same source as the crystal used in the X-ray structure established that the complex had $\mu_{\text{eff}} = 1.40 \mu_{\text{B}}$. This is somewhat smaller than the spin-only moment of 1.73 μ_{B} expected for a low-spin d^7 complex, which has one unpaired electron. No EPR spectrum could be detected for the solid, either at room temperature or at 125 K. We obtained significantly different results for a microcrystalline sample of solid [(4-*t*-BuPy)Co(DH)₂] that we prepared anaerobically following Schrauzer’s procedure.⁴⁸ This solid was diamagnetic within the limits of detection of

the susceptibility balance. A very weak EPR signal was observed for this solid. However, the g values of 2.20 and 2.02 were typical of six-coordinate [Py₂Co(DH)₂] rather than five-coordinate [PyCo(DH)₂].^{50,51} It would appear that the microcrystalline solid is contaminated with trace amounts of six-coordinate complex but is otherwise EPR silent.

Although crystalline and microcrystalline [(4-*t*-BuPy)Co(DH)₂] have different magnetic properties, the solids dissolved to give identical solutions. The EPR spectra of the two solids in toluene and in methylene chloride solution were indistinguishable. At room temperature the spectrum consisted of a broad axial signal that had g values of 2.351 and 2.078. Hyperfine splitting was not observed. The spectrum sharpened sufficiently in frozen solution at 125 K that a third feature could be observed at $g = 2.18$. Each g feature was split by hyperfine coupling to cobalt ($I = 7/2$). In addition, the high-field region exhibited incompletely resolved superhyperfine coupling to one axially bound nitrogen atom ($I = 1$). These spectral features are consistent with those of the five-coordinate complex [PyCo(DH)₂].⁵⁰ The frozen solution spectrum also showed a small extraneous feature near $g = 2.19$ and extra cobalt hyperfine lines in this region, which shows that some six-coordinate [Py₂Co(DH)₂] is also present. Recent studies have demonstrated that the initially formed, five-coordinate [LCo(DH)₂] produced by photolysis of alkylpyridinecobaloximes in frozen matrices redistributes ligands when warmed by abstracting the base from a second molecule to afford six-coordinate [L₂Co(DH)₂] and four-coordinate [Co(DH)₂].⁵⁰ The solution equilibria of [PyCo(DH)₂] are further complicated by dimerization.⁵¹

Complete characterization of the magnetic properties of [(4-*t*-BuPy)Co(DH)₂] solids would require further studies, and is beyond the scope of this investigation. Clearly, the solids are not magnetically dilute systems. The situation is reminiscent of that for cobalt tetraphenylporphyrin, which is found to crystallize in two distinct phases.⁵² One phase is a normal paramagnet and has an EPR spectrum. The second has ferromagnetic exchange coupling resulting in an $S = 1$ ground state and no observable EPR spectrum. Thus, Schrauzer’s and Halpern’s observations may not be contradictory but rather might reflect isolation of different phases of solid [LCo(DH)₂].

Discussion

The results reported here confirm that triphenylstannyl- and triphenylplumbylcobaloxime complexes are readily accessible. Moreover, they are sufficiently robust that their properties and reactivity can be studied in detail. Thus, the exceptional inertness of Co(OEP)SnPh₃ is not specific to that compound, alone, but is a more general phenomenon. In contrast, triphenylgermyl and triphenylsilyl cobaloximes are not accessible in our hands.

(47) Leung, P. C.; Coppens, P. *Acta Crystallogr.* **1983**, B39, 535–542.

(48) Schrauzer, G. N.; Windgassen, R. *J. Chem. Ber.* **1966**, 99, 602–610.

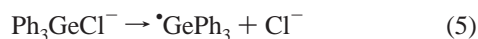
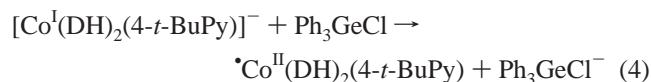
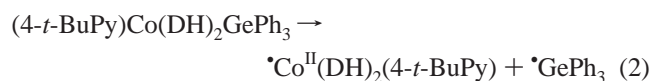
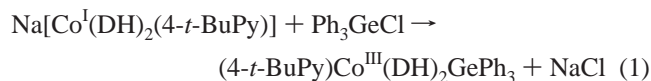
(49) Schneider, P. W.; Phelan, P. F.; Halpern, J. *J. Am. Chem. Soc.* **1969**, 91, 77–81.

(50) Rangel, M.; Leite, A.; Gomes, J.; de Castro, B. *Organometallics* **2005**, 24, 3500–3507.

(51) Rockenbauer, A.; Budó-Záhonyi, E.; Simándi, L. I. *J. Chem. Soc., Dalton Trans.* **1975**, 1729–1737.

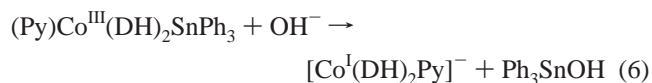
(52) Sato, M.; Kon, H.; Akoh, H.; Tasaki, A.; Kabuto, C.; Silverton, E. V. *Chem. Phys.* **1976**, 16, 405–410.

The triphenylgermyl hydride and cob(II)aloxime products isolated during attempts to prepare the triphenylgermylco-baloxime could result from either of two pathways. In the first mechanism, the expected complex is formed, eq 1, but a weak Co–Ge bond results in facile homolysis, eq 2. Irreversible hydrogen atom abstraction from an unknown donor by the triphenylgermyl radical, eq 3, would afford the hydride product and drive the reversible homolysis reaction, eq 2, to completion. The expected complex is not formed in the second mechanism. A single electron transfer from the cob(I)aloxime to Ph₃GeCl affords a chloride anion and the triphenylgermyl radical, eqs 4 and 5. The latter abstracts a hydrogen atom from a donor to produce the hydride.



It is not clear why our results differ from those of Schrauzer's in the case of the germyl and silylcobaloximes. The difference in the observed solubility of Ph₃GeCl is troubling. It also is possible that one of two changes in reaction conditions is responsible. Schrauzer noted in passing that the stability of the LCo(DH)₂EPh₃ complexes depends on the base component, L, but did not comment on the nature of that dependence.¹⁷ In comparison to pyridine, the stronger donor 4-*t*-butylpyridine might make its cob(I)aloxime anion a stronger reducing agent and enhance pathways such as eqs 3–5. Alternatively, a stronger base might weaken the Co–E bond. However, in the case of alkylcobaloximes, substitution

of a stronger, isosteric base increases the Co–C bond strength.^{53,54} A second difference in reaction conditions was in the choice of reducing agent. Schrauzer employed a greater than 20-fold molar excess of NaBH₄ to reduce the cobaloxime to its cobalt(I) anion. We employed a slight excess of both NaBH₄ and NaOH to affect the same reduction. The hydroxide serves to deprotonate the hydride HCo(DH)₂L to the cobalt(I) anion and thereby prevent H₂ production.⁵⁵ Addition of base eliminates the need for the large excess of NaBH₄ but introduces a potential complication. Addition of OH[−] to a methanolic solution of (Py)Co(DH)₂SnPh₃ results in cleavage of the Co–Sn bond, eq 6.¹⁸ The report of this reaction did not mention what concentration of OH[−] is required for rapid reaction. The good yields of the Sn and Pb cobaloxime complexes establish that loss of product through reaction with OH[−] is not significant under our reaction conditions. The germyl and silyl analogues could be more sensitive to reaction with OH[−], but isolation of cobalt(II) and Ph₃GeH products rather than Ph₃GeOH would appear inconsistent with operation of this decomposition pathway.



Acknowledgment. S.R.W. thanks the General Electric Corp. for a GE Faculty of the Future Grant. We thank the National Institutes of Health (Grant No. GM 33882) and the support of the Eberly College of Arts and Sciences of WVU for support of undergraduate research (S.R.W. and J.E.G.).

Supporting Information Available: X-ray crystallographic files in CIF format. This material is available free of charge via the Internet at <http://pubs.acs.org>.

IC070251+

- (53) Ng, F. T. T.; Rempel, G. L.; Halpern, J. *J. Am. Chem. Soc.* **1982**, *104*, 621–623.
 (54) Ng, F. T. T.; Rempel, G. L.; Mancuso, C.; Halpern, J. *Organometallics* **1990**, *9*, 2762–2772.
 (55) Schrauzer, G. N.; Windgassen, R. J.; Kohnle, J. *Chem. Ber.* **1965**, *98*, 3324–3333.